AIP | Review of Scientific Instruments

Mode-locking optimization with a real-time feedback system in a Nd:yttrium lithium fluoride laser cavity

C. Marengoni, F. Canova, D. Batani, R. Benocci, M. Librizzi, V. Narayanan, M. Gomareschi, G. Lucchini, A. Kilpio, E. Shashkov, I. Stuchebrukhov, V. Vovchenko, V. Chernomyrdin, I. Krasuyk, T. Hall, and S. Bittanti

Citation: Review of Scientific Instruments **78**, 013105 (2007); doi: 10.1063/1.2356853
View online: http://dx.doi.org/10.1063/1.2356853
View Table of Contents: http://scitation.aip.org/content/aip/journal/rsi/78/1?ver=pdfcov
Published by the AIP Publishing

Mode-locking optimization with a real-time feedback system in a Nd:yttrium lithium fluoride laser cavity

C. Marengoni, F. Canova,[a] D. Batani,[a] R. Benocci, M. Librizzi, V. Narayanan, M. Gomareschi, and G. Lucchini
Dipartimento di Fisica "G.Occhialini," Università di Milano Bicocca, Piazza della Scienza 3, 20126 Milano, Italy

A. Kilpio, E. Shashkov, I. Stuchebrukhov, V. Vovchenko, V. Chernomyrdin, and I. Krasuyk
General Physics Institute, Russian Academy of Sciences, 117940 Moscow, Russia

T. Hall
University of Essex, Colchester C04 35Q, United Kingdom

S. Bittanti
Dipartimento di Elettronica & Informazione, Politecnico di Milano via G. Ponzio 34/5, 20133 Milano, Italy

(Received 10 April 2006; accepted 27 August 2006; published online 17 January 2007)

We present a control system, which allows an automatic optimization of the pulse train stability in a mode-locked laser cavity. In order to obtain real-time corrections, we chose a closed loop approach. The control variable is the cavity length, mechanically adjusted by gear system acting on the rear cavity mirror, and the controlled variable is the envelope modulation of the mode-locked pulse train. Such automatic control system maintains the amplitude of the mode-locking pulse train stable within a few percent rms during the working time of the laser. Full implementation of the system on an Nd:yttrium lithium fluoride actively mode-locked laser is presented. © *2007 American Institute of Physics.* [DOI: 10.1063/1.2356853]

I. INTRODUCTION

In this article we describe the measurement and control system designed to stabilize the mode-locking operation of a Nd:YLF (yttrium lithium fluoride) oscillator. The oscillator is part of a 10 TW Nd: glass system in construction at the University of Milano Bicocca, which should finally operate in the 1 ps, 10 J regime using the chirped pulse amplification (CPA) technique.[1–7]

The control of the quality and stability of mode locking is mandatory in order to guarantee a good amplification and experimental reproducibility. In our case, this is particularly true because the laser pulse produced by the oscillator is stretched and chirped in an optical fiber, whose performance strongly depends on the time duration and energy of the input beam, being based on nonlinear effects during propagation.

The cavity detuning problem is well known in literature,[8] because laser systems working in the active mode-locking regime show modulations on the pulse train whenever the frequency of the acousto-optic modulator and the inverse of the cavity round trip time are not perfectly tuned. It is possible to model this behavior using the *self-Q-switching* mathematical model[9] (see also the appendix at the end of the present article). Practically, it is, however, difficult to eliminate all the effects that bring to cavity detuning, since these are due to many different sources (thermal, both in the lasing material and in the acousto-optic modulator, mechanical, etc.) and often show a strong nonlinear behavior.

Therefore we rather chose to implement a *closed loop* approach in order to ensure the stability of the mode-locking pulse train. As explained in more detail in the following, we chose the cavity length as the independent, or *control*, variable (to be mechanically adjusted by a gear system acting on the rear cavity mirror) and the low-frequency modulations of the pulse train envelope as the monitored and measured quantity (the *controlled* variable).

With respect to previous works presented in the literature, our system is characterized by the following key points:

(i) *It uses the low-frequency modulation of the pulse train as the control variable*. With respect to possible alternatives (i.e., monitoring the pulse-to-pulse fluctuations[8]), this allows a deeper insight into the physics of the problem. Moreover it also allows using relatively slow electronics and acquisition devices, which are cheaper and more readily available;

(ii) *It uses a closed loop approach*, without any attempt to directly eliminate all the sources of instabilities (except for the cooling system, as specified later) or any attempt to directly measure the absolute value of the cavity length (which again requires sophisticated and expensive diagnostics);

(iii) *It uses standard components and standard software* (LABVIEW, National Instruments), which can be easily implemented on a personal computer, controlling the full operation of the system, and can be easily adapted and upgraded; and

[a]Also at LOA, Ecole Polytechnique, Palaiseau, France.

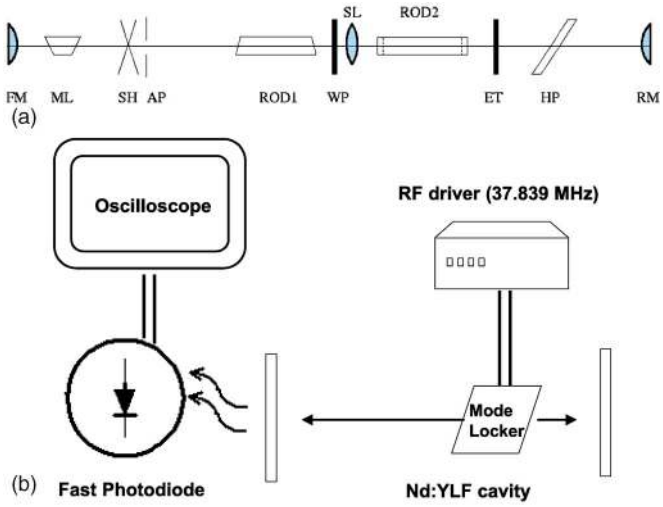

FIG. 1. (Color online) The oscillator cavity (a) and the setup for experimental measurements (b). Here FM is front mirror, RM is rear mirror, AP is intracavity aperture; ML is mode locker; WP is wave plate, ET is etalon, HP is polarizer, SH is pinhole, SL is intracavity focusing lens, and ROD1 and ROD2 are the two (crossed) Nd:YLF rods.

(iv) *It uses a quite robust and fast mathematical model for analysis of the spectra* and the individuation of the main peaks in the low-frequency mode-locking modulations.

In the first part of the article, we describe the experimental observations concerning mode-locking instabilities and their sources (thermal, electronic, and mechanical).

In the second part, we present the solution to the thermal problems.

The third part includes our analysis of the modulation regime and the physical explanation of this behavior.

In the fourth part, we describe the mathematical model and the algorithm we used to measure the instability, which is based on the fast fourier transform and/or the Yule-Walker method.[10]

The fifth part describes the control of the cavity length and the experimental implementation of the system from the hardware and software points of view.

Finally, we present results and conclusions, while the appendix includes a simple model describing mode-locking modulations.[11]

II. OBSERVATION OF MODE-LOCKING INSTABILITIES

Fluctuations and instabilities in the pulse train of mode-locked oscillator have multiple causes and can be described through the self-Q-switching model.[9,12–14] They are characterized by spikes of different amplitudes, which are quite irregular and strongly dependent on cavity detuning. The modulation frequency depends on the mismatch between the natural frequency of the cavity ($c/2L$, where c is the speed of light and L is the effective cavity length) and the mode-locker frequency. The mismatch between the two frequencies may arise from *frequency instability* in the electronic driver of the mode locker (acousto-optic modulator), that brings the system out of resonance, *mechanical vibrations*, usually at very low frequency and poorly dumped, induced by external

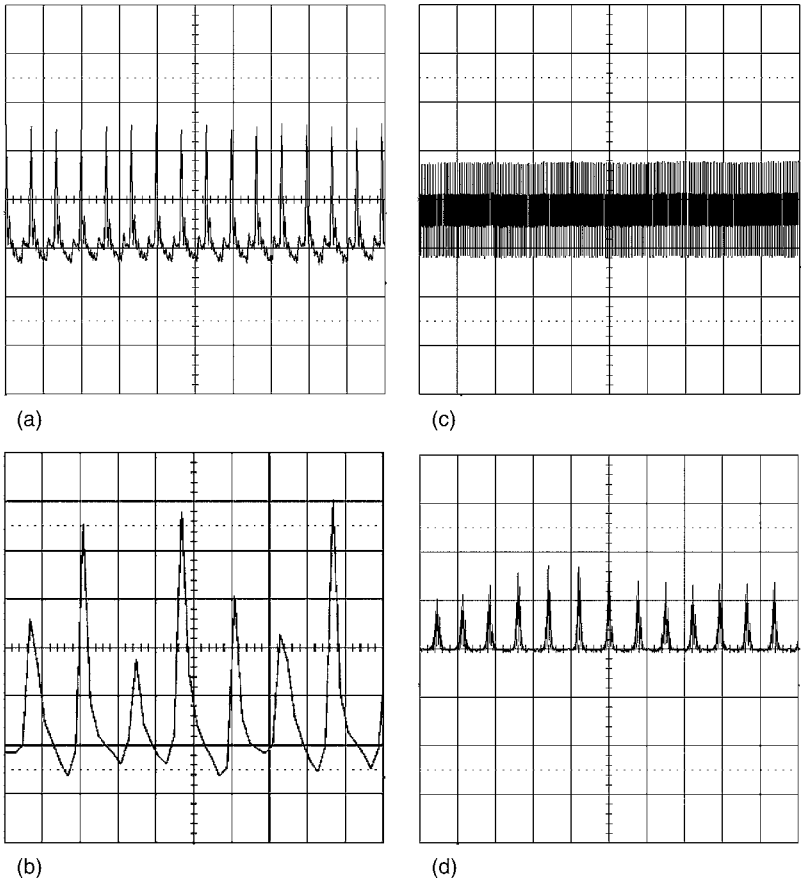

FIG. 2. Example of mode-locked pulse train from the Quantronix oscillator recorded with a digital LeCroy 9344 500 MHz scope and a photodiode type Hamamatsu BPX-65 with 3.5 ns rise time: (a) a few pulses in stable conditions (20 ns horizontal division, 50 mV vertical division), (b) a few pulses in unstable conditions (10 ns horizontal division, 50 mV vertical division), (c) a pulse train in stable conditions (50 μs horizontal division, 100 mV vertical division), (d) a pulse train in unstable conditions (50 μs horizontal division, 1 V vertical division).

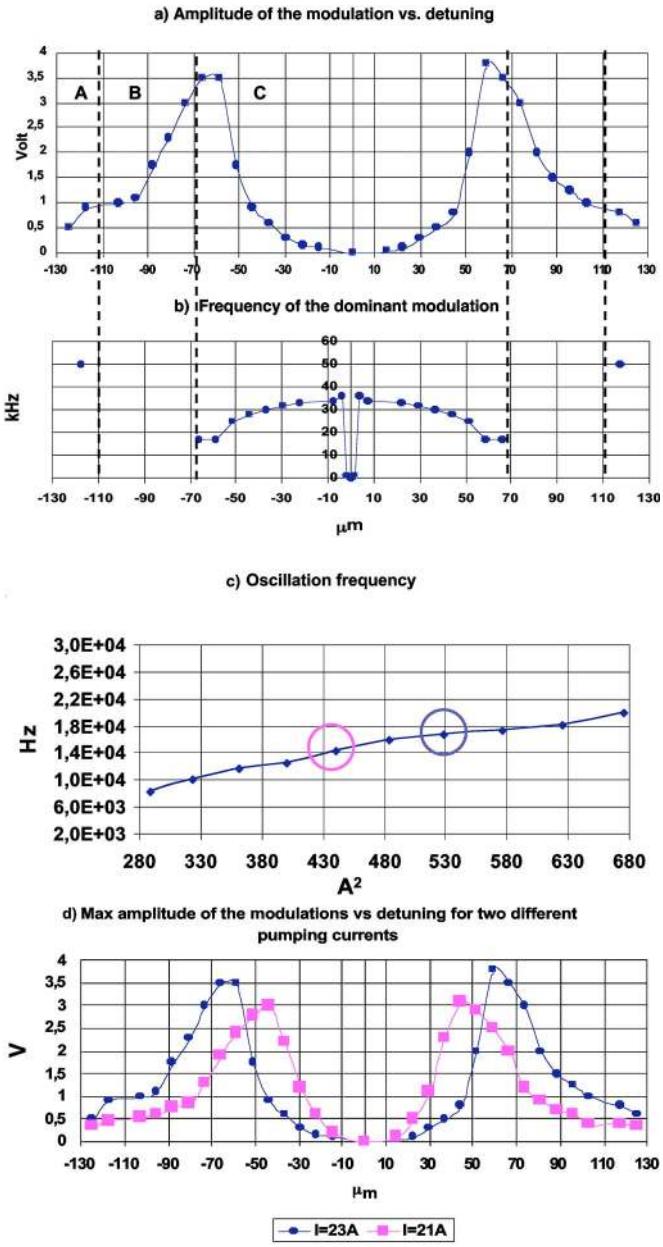

FIG. 3. (Color online) (a) Amplitude modulations of the mode-locking pulse train changing the cavity length (detuning) for a fixed flash lamp current (23 A). Three regions are evidenced: (A) stable pulse train, (B) unstable pulse train with constant frequency carrier, and (C) unstable pulse train with random frequency carrier. (b) Dominant frequency of the modulations in the pulse train vs detuning for a fixed flash lamp current (23 A). (c) Dominant frequency of the modulations vs flash lamp current for a detuning corresponding to the maximum amplitude [for instance the peak in Fig. 3(a) corresponds to an amplitude of 3.8 V and a frequency of 16.8 kHz]. (d) Effect of changing the flash lamp current on the curve shown in Fig. 3(a).

factors (cooling system, air conditioning, and external electric power supply), *thermal load* modulations due to nonhomogeneities in krypton lamps current and insufficient pumping stability, and *insufficient thermal dissipation* on acousto-optic modulator and/or wrong working temperature.

Since it is quite difficult to eliminate all the sources of instability (except the working temperature of the acousto-optic modulator) we opted for a closed loop approach in order to control and stabilize the mode-locking pulse train.

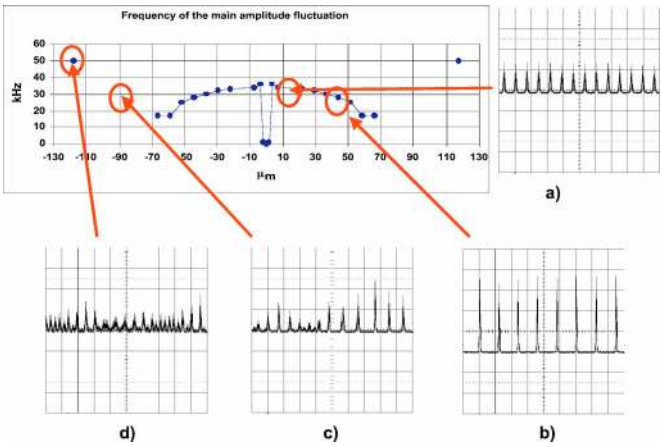

FIG. 4. (Color online) Different behaviors induced by the detuning on mode locking: unstable pulse train with constant frequency carrier [(a) and (b)] and unstable pulse train with random frequency carrier [(c) and (d)].

A. The Nd:YLF oscillator

The oscillator is a Quantronix Model 4216D cw mode-locked laser with crossed double-rod Nd:YLF, pumped by flash lamps, working at high repetition rate (≈80 MHz) (Fig. 1). Each of the two active material rods, 4 mm in diameter and 79 mm long, is pumped by a single krypton arc lamp placed in an elliptical gold-coated cavity. The output coupler [FM in Fig. 1(a)] has a transmission of 12%. The laser operates in the TEM_{00} transverse mode thanks to an intracavity aperture [AP in Fig. 1(a)]. The system was designed to eliminate thermal lensing effect by a particular positioning of the Nd:YLF rods.[15] The mode locker (ML) is driven by a rf power of 8 W at ≈40 Mhz. It creates a pulse train with pulse width of 100 ps and a peak power of 10^4 W/cm^2.

Figures 2(a)–2(d) show examples of mode-locked pulse trains produced by the Quantronix oscillator recorded with a digital LeCroy 500 MHz 9344 oscilloscope and a photodiode type Hamamatsu BPX-65 with 3.5 ns rise time. Pulses are observed on a 5 ns time scale in (a) stable and in (b) rather unstable conditions (showing very large pulse-to-pulse fluctuations). Let us notice that the temporal resolutions of the oscilloscope and of the used detector are not sufficient to measure the temporal duration of the single pulses. However they are suitable for checking the pulse train stability, i.e., the amplitude of single pulses and the pulse repetition frequency.

Figures 2(c) and 2(d) shows mode-locked pulse trains produced by the oscillator, (c) in stable conditions and (d) when the instabilities are present. Here we used a longer time scale (50 μs), which allows evidencing the long-time modulations of the pulse train, with typical frequencies in the 0–30 kHz range.

III. DETAILED CHARACTERISTICS OF MODE-LOCKING INSTABILITIES: PARAMETRIC STUDY

In order to obtain a complete overview of the problem of mode-locking instabilities, we performed a parametric study on the possible sources of instability.

We first identified the frequency shift of the radio frequency driver of the mode locker, the mechanical perturbations (vibrations), and the thermal load on the laser as pos-

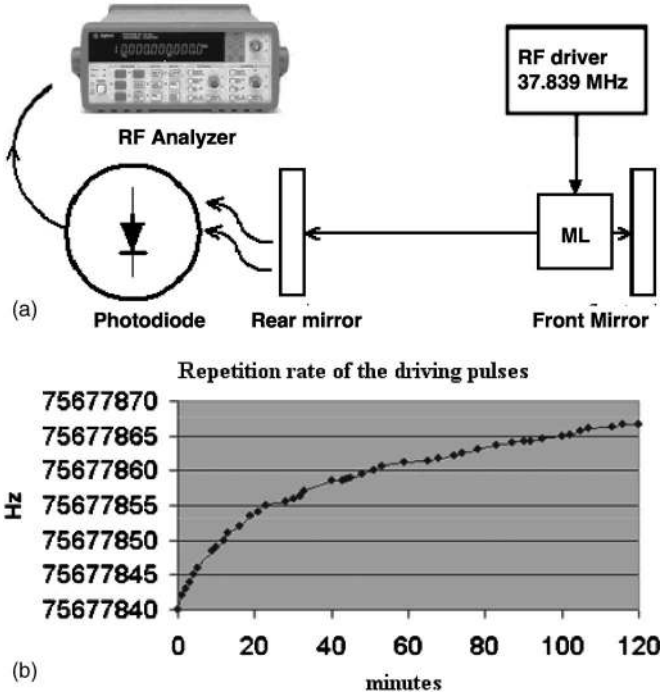

FIG. 5. Setup of the experiment to test the stability of the rf driving signal (a), and frequency drift for 2 h of measurement (b).

sible sources of instabilities. Then, for characterizing such instabilities, we measured the amplitude of the modulation in the mode-locking pulse train while changing the cavity length and the current applied to the laser flash lamps. Our experimental results are shown in Fig. 3.

A. Measurement of the amplitude modulations changing the flash lamp current and the cavity length (detuning)

The amplitude of the modulations is defined as the peak-to-valley (PV) value of the spikes present in the envelope of the mode-locking pulse train. These are low frequency and may have large amplitude [eight to ten times the average pulse amplitude, compare Figs. 2(c) and 2(d)].

Such modulations appear after the system has been operational for some time. When they appear, one needs to manually adjust the laser cavity, even as frequently as every half an hour.

The amplitude and the frequency of the modulations of the mode-locked pulse train were studied while changing the cavity length (detuning) while keeping the flash lamp current constant. The maximum detuning was ±120 μm. We can recognize three different regimes (Fig. 4):

(A) *Stable mode locking* (detuning of ± a few microns): The pulse train shows no appreciable modulations [Fig. 2(c)].

(B) *Modulations with a constant carrier frequency* (detuning of less than ±50 μm): In this zone the pulse train is modulated with a dominant frequency, which smoothly shifts from 30 to 15 kHz.

(C) *Modulations with unstable (random) carrier frequency* (detuning between +60 and +120 μm and between −60 and −120 μm): In this zone the mode-locking regime is very unstable and the oscillation frequency of the modulations of the pulse train envelope changes every few cycles.

Figure 3(d) shows that for two different fixed flash lamp currents, the detuning behavior is similar and the different zones still exist, only the width of the stability zone and of unstable regions change.

B. Sources of mode-locking instability

The possible reasons for the mode-locking instabilities are the drifting of the rf driving signal, mechanical resonances, coming from the pump of the water cooling system and the environment of laboratory and an insufficient evacuation of the thermal load from the Nd:YLF rods, insufficient heat removal from the mode-locking crystal, and misaligned cavity length.

1. Experimental measurement of the frequency drift of the rf signal

To test the stability of the frequency of the rf driver of the mode locker we measured the repetition frequency of the laser pulses with a frequency analyzer (1 mHz resolution) for 2 h, using the experimental setup in Fig. 5(a). Also, we used a two-channel rf analyzer to simultaneously measure the repetition frequency of the laser pulses (as shown in figure) and the rf driving frequency.

The measurements showed that the two signals were shifting in time while keeping an exact ratio of 2 (as expected) at all times. Therefore we can conclude that the shift in the pulse repetition frequency is without any doubt induced by the frequency of the rf driving signal.

Figure 5(b) shows that the electronics components of the driver are affected by a drift of about 30 Hz during such 2 h time period and seems to slowly approach an asymptotic value. Such drift can be fitted with a logarithmic slope, in agreement with the usual thermal drift in electronics components.[16]

2. Mechanical resonances and thermal load

The laser is mounted on an INVAR breadboard, designed to dump low frequency (1–100 Hz frequency) and with a thermal coefficient of dilatation of 200 nm/K. From this point of view we are quite sure that the alignment is robust and none of the modulations come from these sources.

Moreover, this particular oscillator is practically insensitive to thermal load, thanks to the specific design, which uses two rods plus a converging lens configuration for eliminating thermal lense effects.[15]

3. Heat on the mode-locking crystal: External cooling system

The laser system was characterized by an undesired coupling between the cooling system of the acousto-optic modulator and that of the flash lamps and lazing rods, which use the same water. This serial configuration must be considered as a serious design fault: indeed, whenever the laser is operated for sufficiently long time, the water warms up, and the temperature of the acousto-optic modulator is not kept

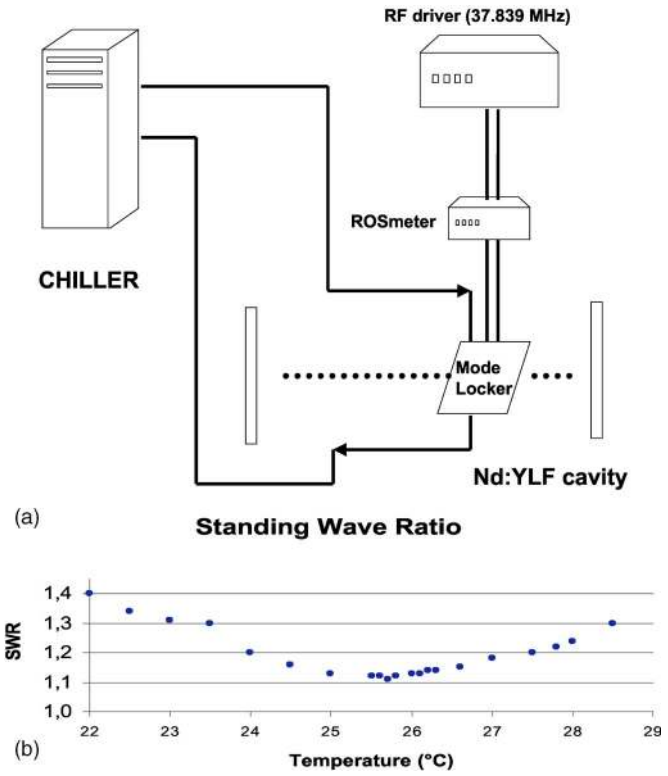

FIG. 6. Setup used to independently control and optimize the temperature of the mode-locker crystal (a), standing wave ratio (SWR) of the acousto-optic modulator vs thermal bath temperature (laser working with the flash lamp current fixed at 23 A).

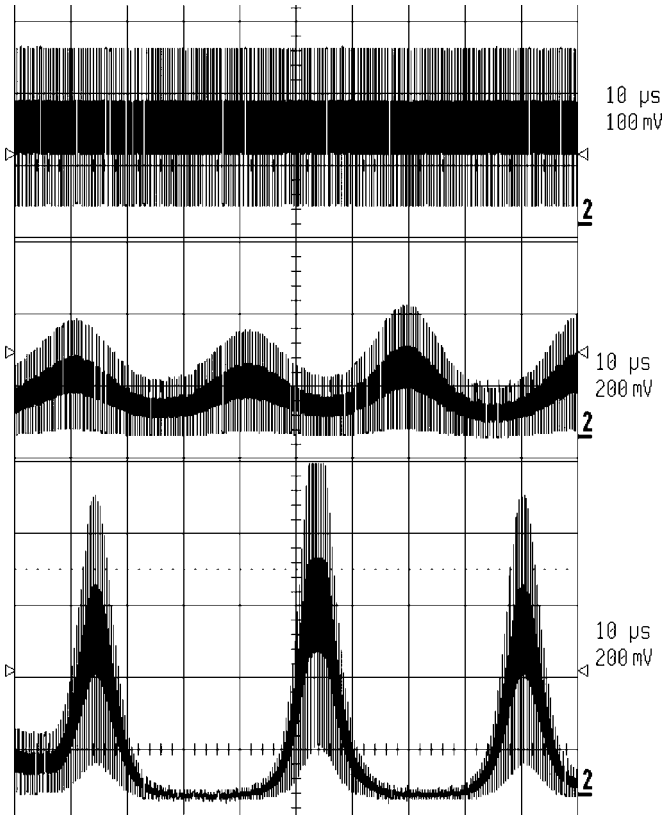

FIG. 7. Time evolution of the mode-locked pulse train on long time scales (first image on the top: time $t=0$, 10 μs horizontal division, 100 mV vertical division; intermediate image: $t=+30$ min, 10 μs horizontal division, 200 mV vertical division; and last image on bottom: $t=+60$ min, 10 μs horizontal division, 200 mV vertical division). The laser was working with a flash lamp current of 23 A. The implementation of the separate temperature control of the mode locker improved the stability of the system from $\approx$20 to $\approx$90 min.

constant. While this is not a big problem for the working conditions of the flash lamps and lazing rods, the acousto-optic modulator should instead work at fixed temperature conditions.[17]

Therefore we implemented a separate cooling system for the modulator by using a cooling bath, type Huber Polystat k6, which allows a temperature control at ±0.1 °C. The working point of the modulator was set by measuring the energy reflected by the crystal back into the driver [standing wave ratio (SWR)], with a rosmeter (Diamond SX-200). Figure 6(b) shows the experimentally measured SWR versus temperature showing an optimal working temperature of 25.7±0.6 °C.

The implementation of the separate temperature control of the mode locker did definitely improve the reliability of the system: the stability time increased from $\approx$20 to $\approx$90 min. However, after this time, the modulations and the unstable operations appears again (see Fig. 7). Indeed getting longer stability times required the implementation of the closed loop automatic system for cavity control.

C. Relaxation oscillations

Relaxation oscillations are well known in literature[11] as low-frequency modulations due to energy exchange between the radiation in the cavity and the energy stored in the active medium. These are particularly relevant for lasing materials with long decay times, as it is the case of Nd:YLF (about 450 μs). The typical frequency of relaxation oscillation can be expressed as

$$f_n = \frac{\sqrt{(P/P_{\text{th}} - 1)/\tau_{\text{cavity}}\tau_{\text{fluo}}}}{2\pi}, \tag{1}$$

where P is the pump power, proportional to I^2 (I is the current driving the flash lamps, and the emission of the gas discharge is proportional to $P=I^2R$, the Joule law), P_{th} is the power threshold necessary to get lasing in the cavity, and τ_{cavity} and τ_{fluo} are the cavity life time and the decay time of the inverted population.

In our case, the observed large oscillations in the mode-locked pulse train may indeed be due to relaxation oscillations triggered by the various sources we just described (rf

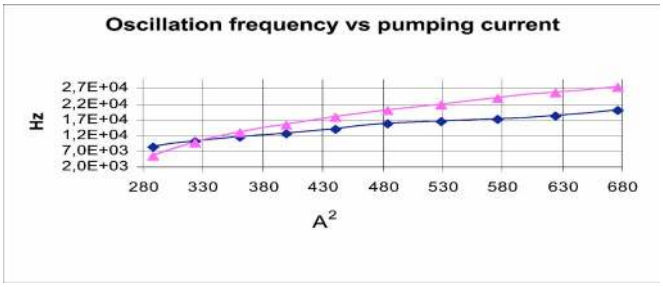

FIG. 8. (Color online) Modulation frequency vs driving currents in the flas hlamps (blue curve, diamonds), showing a fair agreement with the slope (pink curve, triangle) calculated with formula (1).

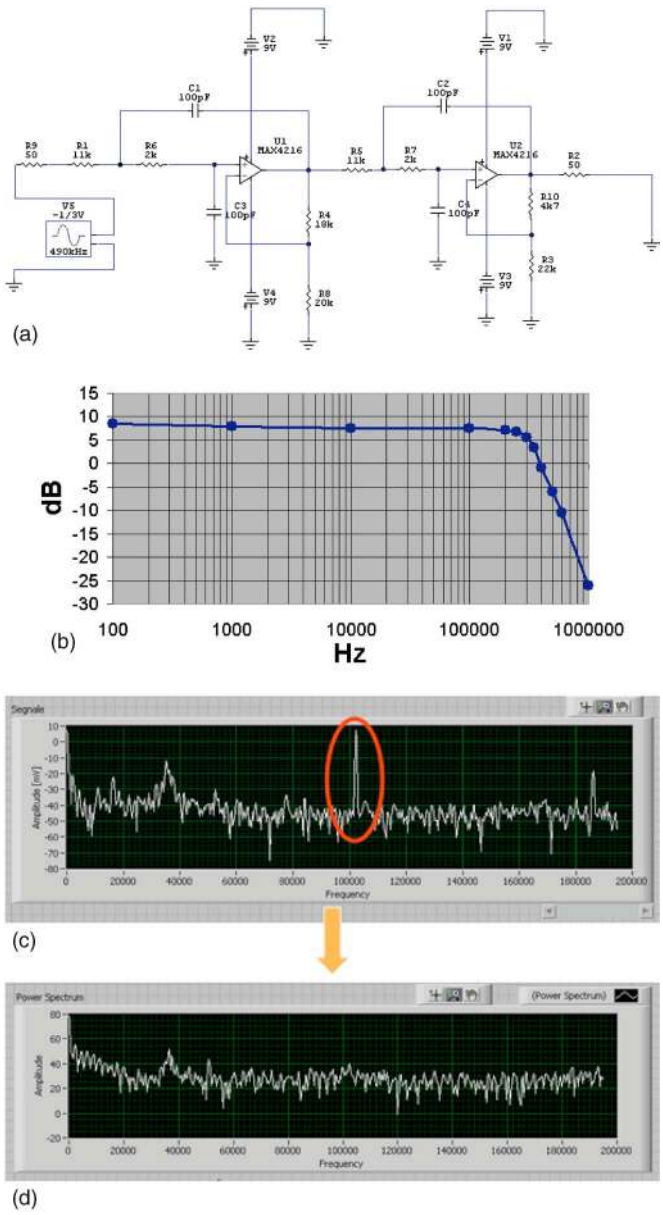

FIG. 9. (Color online) Electronic scheme of the Sullen-Kay filter, the filter response, calculated with the SPICE software, and the signal (spectrum of modulations measured with the ADC and obtained with FFT) with (c) and without (d) the base band replica.

drift, heat problems, etc.). These induce a detuning between the cavity frequency $(c/2L)$ and the acousto-optic modulator frequency, which produces a low-frequency beating. Whenever such beating has a frequency close enough to the frequency of relaxation phenomena, we fall in resonance, and we expect the onset of very large oscillations in the mode-locked pulse train.

In order to test this scenario, we measured the main (dominant) frequency of the modulations versus the driving current in the flash lamps (see Fig. 8). The behavior is in fair agreement with what can be calculated using formula (1), suggesting indeed the role of relaxation oscillations in the observed phenomena.

Finally let us notice that the observed frequency shift corresponds to an induced cavity detuning of the order of

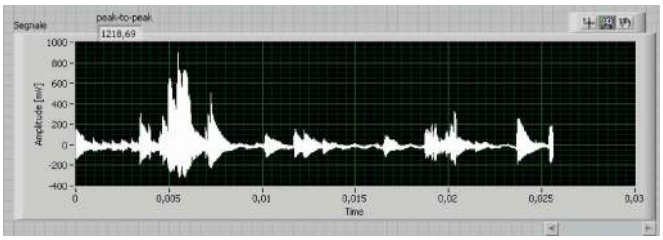

FIG. 10. Typical signal acquisition from the ADC.

$$\Delta L = \left| \frac{c}{2\upsilon_f} - \frac{c}{2\upsilon_i} \right| \cong 1\ \mu\text{m}, \tag{2}$$

with υ_f and υ_i as natural frequency of the cavity $(c/2L)$ and the relaxed frequency [see Fig. 5(b) for instance]. Such estimated detuning is in qualitative agreement with the measurements shown in Sec. III A.

IV. NUMERICAL METHODS: YULE-WALKER ALGORITHMS AND FAST FOURIER TRANSFORM

As previously explained, we choose to find the control variable in the transformed space in order to fully estimate the effect of the beating between the mode-locker and cavity frequencies. Two algorithms allow us to follow the dynamic of modulations: the *fast Fourier transform* and the *Yule-Walker method*.

The fast Fourier transform algorithm, executing the discrete Fourier transform (DFT) of a signal, is a well known technique in signal processing, which is very robust from the numerical point of view, but strongly dependent on the number of available samples as far as noise rejection is concerned.

In our experiment, we initially used this method for acquiring data with a fast photodiode and a large bandwidth oscilloscope.

Then, in order to realize a closed loop system using the fast fourier transform (FFT) method and a commercial analog/digital converter (ADC), we used the undersampling technique, a windowing function, and an analogical double Sullen-Key filter (Butterworth, 4°, see Fig. 9). The role of the filter was to act as antialiasing, in the bandwidth from 0 to 300 kHz. The Sullen-Key filter used two operational amplifiers (OAs) of the type EL2045 (with $B=100$ Mhz and SR$=275\ \mu$V/s).

The Yule-Walker method is a powerful parametric tool for fitting AutoRegressive models to data. From such models, the spectrum can be obtained along a different route and compared with that deduced via FFT. The advantage is that the methods appear to be more robust against noise corrupting data. Figures 10 and 11, respectively, show the typical signal acquisition from the ADC and the corresponding spectra obtained with the FFT and the Yule-Walker method.

To use this algorithm efficiently, we designed a data acquisition system composed by a fast photodiode (3.5 ns rise time), an ADC (Picotech212/50, 50 Msps, 12 bit, ±1% accuracy), and a LABVIEW VI, which realizes the matrix inversion.

The noise rejection characteristic of this method allows us to easily identify the frequency created by the beating in the cavity.

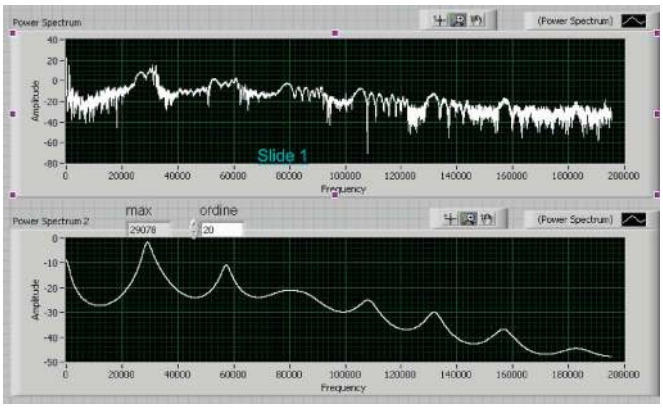

FIG. 11. (Color online) FFT (up) and Yule-Walker (down) spectral estimations.

Its only drawback is the fact that the implementation of this method slows the software down. However, this is not a major problem in our case because our system does not require a fast correction (the instability grows over a time scale of 10 min; therefore cavity length adjustments can be operated within a few minutes).

V. CONTROL OF THE CAVITY LENGTH: INSTRUMENTAL IMPLEMENTATION

Continuously changing the cavity length, in order to follow the changes in the modulation frequency in real time, is a well-known technique, already presented in scientific literature,[9] used to eliminate any modulation in the mode-locking behavior in the detuning of the laser cavity itself. This technique consists in continuously changing the cavity length so as to have a real time correction to follow changes in the modulation frequency.

Such changes are the result, as we have seen above, of slow phenomena (period of minutes), so it is affordable to execute cavity length corrections with a mechanical system, which is very slow compared to the typical times of a laser system (pulse duration less than a nanosecond). The system works in a closed loop mode (see Fig. 12), the optical signal acquired by a photodiode is sampled by an ADC and undergoes a low-pass filtering with a double Sullen-Key. Finally, a

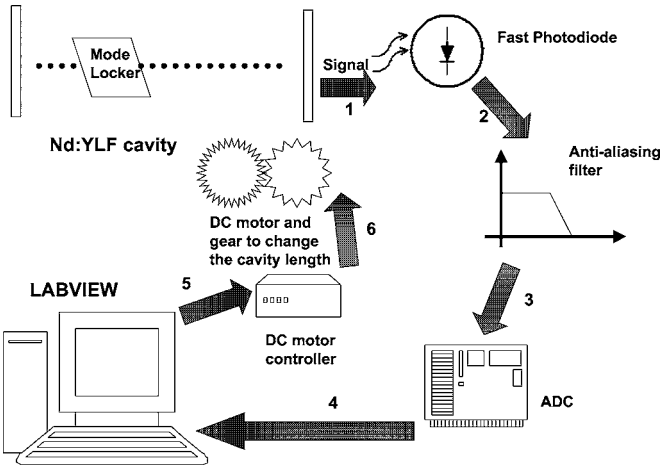

FIG. 12. Scheme of the closed loop system for the automatic control of the laser cavity length.

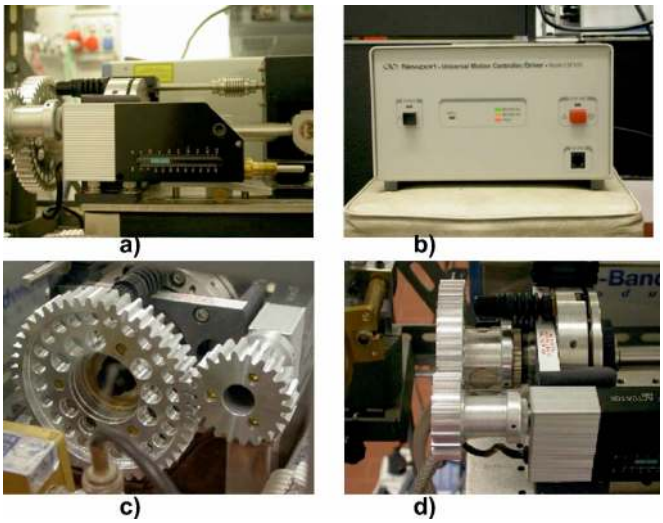

FIG. 13. (Color online) Driver (a), micrometric motor (b), and gears used to implement the cavity length control moving the rear mirror of the laser cavity [(c) and (d)].

LABVIEW routine extracts its frequency. The LABVIEW VI activates a mechanical gear system and the cavity length is changed, following an experimental control law, until the modulation is eliminated.

The goal of such cavity length control system was to assure stable working conditions right from the laser switch on up to the end of the working time, avoiding the need for waiting for a very long time (as usually done in laser laboratories) while waiting, for instance, that the rf driver has stabilized. It also allows compensating for other sources of instabilities. In the practical realization we opted for a system which is modular and hence it can be easily reconfigured, a "user-friendly" interface, and the choice of control variables at low frequencies.

A. Hardware: Mechanical and electronic system

The components of the mechanical systems are shown in Fig. 13. It includes (1) a driver (ESP 100) and a linear dc motor (Newport 850F DC), characterized by an accuracy of the linear position of 1 μm and by a screw tap of 1.275 rounds/mm and (2) a movement transmission made of two cylindrical gear wheels with module 2 (and, respectively, gear numbers of 48 and 24).

B. Control law and cavity length correction algorithm

The control law is based on the analysis of the envelope of the pulse train. The control variables are the *frequency* and the *amplitude* of the modulations, and the control function $\alpha=f(y_1,y_2,I)$ defines the look-up table used to choose the action and correct the detuning (see Fig. 14). This control law is valid for a detuning length between two maxima (zone with modulations with a constant carrier frequency,±50 μm, of the cavity length, Fig. 4(c)).

C. The Role of LABVIEW in the control system

LABVIEW VI (National Instruments) represents the software link between the data acquisition, from the ADC, and the control of the cavity length driving a dc linear motor. The

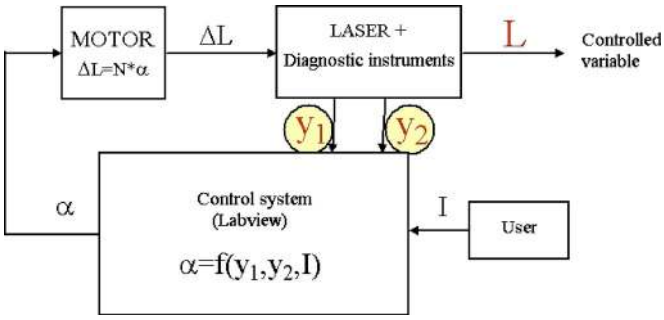

FIG. 14. (Color online) Control diagram for the control law $\alpha=f(y_1,y_2,I)$: α is the motor angle, L is the cavity length and ΔL is the detuning, I is the current in the pump flash lamps, y_1 is the modulation amplitude, and y_2 is the modulation frequency.

steps executed by LABVIEW are digital signal acquisition and analysis (FFT and Yule-Walker algorithms), computation of the look-up table using the control law, and control of the electromechanical devices to correct the cavity length.

VI. DISCUSSION

In this article we have shown the measure and control system that we have developed to eliminate modulation on the mode-locking pulse train in Nd:YLF laser oscillator.

This system measures the frequencies present in the modulated mode locking and adjusts the length of the cavity via a mechanical gear system. This system works with a feedback (closed loop) approach and guarantees a stable mode locking.

ACKNOWLEDGMENTS

We thank S. Coppola, G. Martello, and M.Cavallotti from the University of Milano Bicocca for their invaluable help in setting up the laboratory.

APPENDIX: MODEL OF MODE-LOCKING MODULATION BEHAVIOR AND SIMULATION RESULTS

In the case of small amplitudes, the modulations of the mode-locking pulse train can be described using the self-Q-switching model.[9–14] Here, the beating between the acousto-optic mode-locker frequency and the natural cavity frequency excites some almost-sinusoidal and exponentially dumped modes of the system. These are typical of solid-state lasers, where the fluorescence time ($\tau_{\text{fluo}}=450\ \mu$s for Nd:YLF) is much longer than the round-trip time in the laser cavity (around 10 ns for typical oscillators). The applicability of this model in our configuration in confirmed by the fair fit of numerical predictions with experimental data (as shown in Fig. 8).

Relaxation oscillations are described by coupled rate equations, which must be numerically solved. An approximated formula for the pulse behavior is

$$n(t) = n + n_1 \exp(-\gamma t)\cos(\omega t),$$

where γ is the decay rate ($\gamma=x/\tau_{\text{fluo}}$) and ω is the relaxing frequency $\omega=[x/(\tau_{\text{fluo}}\tau_{\text{cavity}})]^{1/2}$. For our cavity $\tau_{\text{fluo}}=500\ \mu$s, $x=4$, and $\tau_{\text{cavity}}=1\ \mu$s, so that $\gamma=4/(500\ \mu\text{s}) \approx 1/(100\ \mu\text{s})$ and $\omega=[\approx 4/(500\times 1\ \mu\text{s}^2)]^{1/2}\approx 30$ kHz.

Experimentally we see that the system is characterized by a main (dominant) frequency ω but also by secondary frequencies, and we observe that the main frequency changes in time. This behavior can be explained with a slightly more complex model for the resonance oscillations, where

$$n(t) = n + n_1 \exp(-\gamma t)\cos(\omega_1 t),$$

with

$$\omega_1 = (\omega^2 - \gamma^2)^{1/2},$$

$$\omega = [(x-1)/(\tau_{\text{fluo}}\tau_{\text{cavity}})]^{1/2},$$

$$\gamma = x/\tau_{\text{fluo}}.$$

In this way, the cavity losses (γ) are included in the formula defining the modulation frequency (ω_1). Since the cavity losses are dependent on any disturbing phenomena appearing in the laser (thermal, mechanical, etc.), this explains the time changes of the main frequency and the appearance of secondary frequencies.

[1] D. Strickland and G. Mourou, Opt. Commun. **56**, 219 (1985).
[2] P. Maine, D. Strickland, P. Bado, M. Pessot, and G. Mourou, IEEE J. Quantum Electron. **24**, 398 (1988).
[3] E. B. Treacy, IEEE J. Quantum Electron. **5**, 454 (1969).
[4] N. B. Nikolaus and D. Grischkowsky, Appl. Phys. Lett. **42**, 1 (1983).
[5] R. Wolleschensky and J. Mühlsteff, Ph.D. thesis, University of Essex, 1996; F. Canova *et al.*, Radiat. Eff. Defects Solids **160**, 669–675 (2005).
[6] O. E. Martinez, IEEE J. Quantum Electron. **23**, 1385, (1987).
[7] D. Descamps, Ph.D. thesis, Ecole Polytechnique, 1997.
[8] H. J. Eichler, W. Filter, and T. Weider, IEEE J. Quantum Electron. **24**, 1178 (1988).
[9] Y. M. John and H. J. Kong, IEEE J. Quantum Electron. **29**, 1042 (1993).
[10] S. M. Savaresi, S. Bittanti, and H. C. So, IEEE Trans. Autom. Control **48**, 7 (2003); S Bittanti, *Model Identification and Adaptive and Adaptive Systems*, in Italian, Pitagora Editrice, Bologna (2004).
[11] A. Siegman, *Lasers* (University Science Books, Sausalito, CA, 1986).
[12] J. J. O'Neil and J. N. Kutz., IEEE J. Quantum Electron. **38**, 1412 (2002).
[13] H. Statz, G. DeMars, D. Wilson, and C.. L. Tang, J. Appl. Phys. **36**, 1510 (1965).
[14] N. Joly and S. Bielawski, Opt. Commun. **220**, 171 (2003).
[15] H. Vanherzeel, Appl. Opt. **27**, 17 (1988).
[16] P. Horowitz, *The Art of Electronics* (Cambridge University Press, Cambridge, 1980).
[17] O. Svelto, *Principles of Lasers*, 4th ed. (Springer, New York, 1998).